

Leucinostatin Y: A Peptaibiotic Produced by the Entomoparasitic Fungus *Purpureocillium lilacinum* 40-H-28

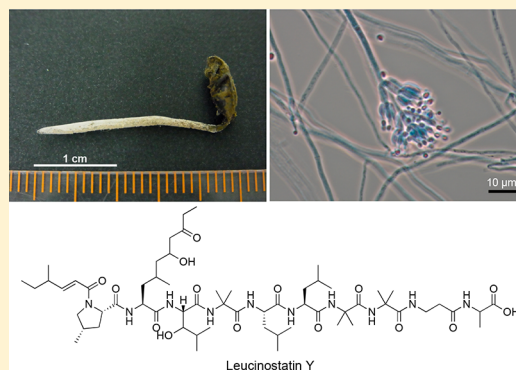
Isao Momose,^{*,†} Takefumi Onodera,[†] Hiroyasu Doi,[†] Hayamitsu Adachi,[†] Masatomi Iijima,[†] Yohko Yamazaki,[†] Ryuichi Sawa,[‡] Yumiko Kubota,[‡] Masayuki Igarashi,[‡] and Manabu Kawada^{†,‡}

[†]Institute of Microbial Chemistry (BIKAKEN), Numazu, 18-24 Miyamoto, Numazu-shi, Shizuoka 410-0301, Japan

[‡]Institute of Microbial Chemistry (BIKAKEN), Tokyo, 3-14-23 Kamiosaki, Shinagawa-ku, Tokyo 141-0021, Japan

Supporting Information

ABSTRACT: Leucinostatin Y, a new peptaibiotic, was isolated from the culture broth of the entomoparasitic fungus *Purpureocillium lilacinum* 40-H-28. The planar structure was elucidated by detailed analysis of its NMR and MS/MS data. The absolute configurations of the amino acids were partially determined by an advanced Marfey's method. The biological activities of leucinostatin Y were assessed using human pancreatic cancer cells, revealing the importance of the C-terminus of leucinostatins for preferential cytotoxicity to cancer cells under glucose-deprived conditions and inhibition of mitochondrial function.



Solid tumors contain large areas that are nutrient- and oxygen-deprived due to the immaturity and irregular distribution of blood vessels therein.^{1,2} Certain cancer cells have an inherent ability to tolerate harsh growth conditions, such as nutrient and oxygen deprivation, and can survive for prolonged periods of time.³ To survive in a nutrient-limited environment, cancer cells utilize the PI3K-AKT-mTOR pathway and the unfolded protein response.^{3–5} Kigamicins, which are polycyclic xanthenes isolated from the culture broth of *Amycolatopsis* sp. ML630-mF1, inhibit activation of Akt and exhibit preferential cytotoxicity to cancer cells under nutrient-deprived conditions compared to those under nutrient-rich conditions.^{6–8} Versipelostatin, a 17-membered macrocyclic compound isolated from the culture broth of *Streptomyces versipellis* 4083-SVS6, suppresses activation of the unfolded protein response and shows highly selective cytotoxicity to glucose-deprived cancer cells.^{9,10}

Targeting nutrient-deprived cancer cells is an attractive strategy for cancer therapy. Therefore, our research has focused on screening cytotoxic agents that act preferentially under nutrient starvation. In previous studies, we found that inhibitors of mitochondrial functions such as leucinostatin A (**1**, an inhibitor of mitochondrial ATPase) exhibit preferential cytotoxicity against cancer cells adapted to nutrient-starved conditions.¹¹

Microbial metabolites are a rich and promising source of drug candidates. In the early years of antibiotic studies, approximately 60% of all bioactive microbial metabolites were isolated from actinobacteria.¹² However, the significance of fungi as secondary metabolite producers has continuously increased, accounting for 61% of all bioactive microbial

metabolites discovered in the period 2001–2010. We are particularly interested in entomoparasitic fungi, including the most well-known insect pathogenic fungus *Cordyceps sinensis*, because they are rich sources of novel biologically active substances with diverse structural architectures.^{13,14} Therefore, we screened the metabolites of entomoparasitic fungi to identify agents that preferentially reduce the survival of nutrient-deprived cancer cells and identified a new peptaibiotic¹⁵ named leucinostatin Y (**2**), which is produced by *Purpureocillium lilacinum* 40-H-28 (Figure 1).

A number of leucinostatins have been identified in previous studies. Although the structures of leucinostatins have been elucidated by tandem mass spectrometry (MS/MS), X-ray diffraction, and chemical degradation,^{16–21} the ¹H and ¹³C NMR signals for leucinostatins have not been assigned. Therefore, we assigned the ¹H and ¹³C NMR spectra for leucinostatins A (**1**) and Y (**2**). In this report, we describe the isolation, structural elucidation (including NMR assignment), and biological evaluation of **1** and **2**.

RESULTS AND DISCUSSION

The entomoparasitic fungus *P. lilacinum* 40-H-28 was isolated from the synnema formed on *Macroscytus japonensis* Scott²² collected at Yokohama City, Kanagawa Prefecture, Japan. *P. lilacinum* 40-H-28 was cultured in a liquid medium (16 L), and the filtrate obtained from the cultured broth was applied to a Diaion HP-20 column. The active fractions eluted with

Received: October 10, 2018

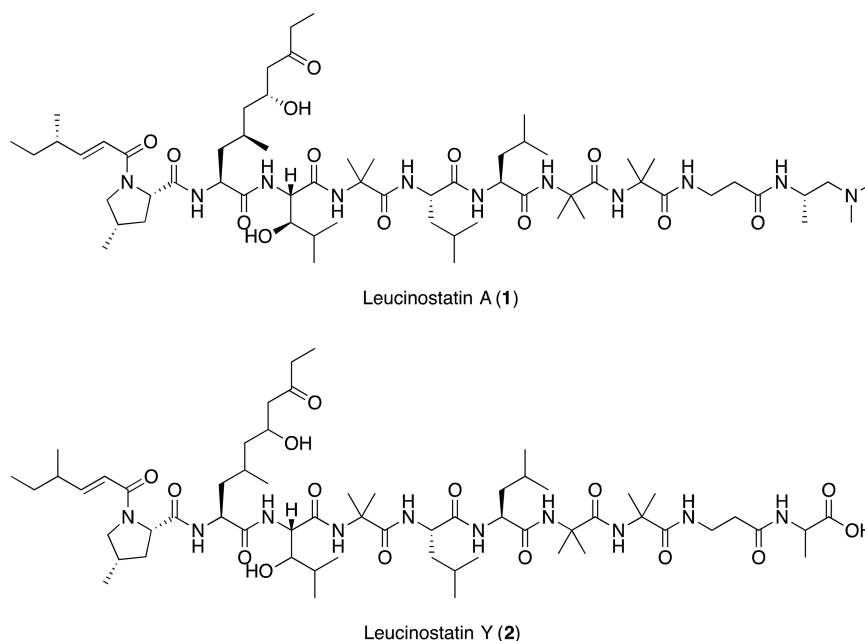


Figure 1. Structures of leucinostatins A (1) and Y (2).

acetone were concentrated to give an oily material. The resulting material was applied to a silica gel column and a Sephadex LH-20 column, followed by HPLC to afford the new peptaibiotic leucinostatin Y (2), together with the known peptaibiotic leucinostatin A (1).

Leucinostatin A (1) was first isolated from the culture broth of *Penicillium lilacinum* by Arai et al.²³ Abe et al. reported the total synthesis of 1 and revealed its correct structure in 2017.²⁴ We obtained 1 as a colorless, amorphous solid. The molecular formula of 1 was confirmed to be C₆₂H₁₁₁N₁₁O₁₃ by high-resolution electrospray ionization mass spectrometry (HRESIMS). Spectroscopic data of natural 1 are identical to those of synthetic 1.²⁴ ¹H and ¹³C NMR signals of natural and synthetic 1, however, have never been assigned to the appropriate protons and carbons. Therefore, we assigned the ¹H and ¹³C NMR data of 1 using a similar approach to that for 2, which is shown below (Table 1).

Leucinostatin Y (2) was obtained as a colorless, amorphous solid. The UV spectrum of 2 exhibits absorption maxima at 205 and 223 nm and is very similar to that of 1.²³ The molecular formula of 2 was determined to be C₆₀H₁₀₄N₁₀O₁₅ based on HRESIMS and ¹H and ¹³C NMR analysis, indicating that 2 has two fewer carbon atoms, seven fewer hydrogens, one fewer nitrogen, and two additional oxygen atoms than 1. The planar structure of 2 was primarily elucidated using NMR experiments. The assignments of the ¹H and ¹³C NMR data (Figures S1 and S2) for 2 are shown in Table 1. The ¹³C NMR and DEPT data (Figure S3) along with the HSQC spectra (Figure S4) revealed the presence of 60 carbons in 2, which were categorized as 18 methyl, 11 methylene, 14 sp³ methine, two sp² methine, three N-substituted tertiary, and 12 carbonyl carbons. The ¹H NMR and HSQC spectra revealed the presence of nine amide protons. The COSY spectrum shows correlations between coupled protons (Figure S5), the HSQC-TOCSY spectrum shows correlations between all protons within a given spin system (Figure S6), and the HMBC spectrum reveals long-range correlations between protons and carbons in 2 (Figure S7). These data indicate the presence of 4-methyl-2-hexenoic acid, 4-methylproline (MePro), 2-amino-

6-hydroxy-4-methyl-8-oxodecanoic acid (AHMOD), β -hydroxy-leucine (HyLeu), three 2-aminoisobutyric acid (Aib), two leucine (Leu), β -alanine (β -Ala), and alanine (Ala) residues in 2 (Figure 2). Thus, 2 possesses an Ala residue instead of the N¹,N¹-dimethylpropane-1,2-diamine moiety of 1. The sequence of amino acid residues in 2 was established by the HMBC spectrum, which reveals correlations between the carbonyl carbon (δ_C 168.3) of the 4-methyl-2-hexenoic acid moiety and the α -methine proton (δ_H 4.32) of MePro, the carbonyl carbon (δ_C 175.9) of MePro and the NH proton (δ_H 8.55) of AHMOD, the carbonyl carbon (δ_C 176.6) of AHMOD and the NH proton (δ_H 7.91) of HyLeu, the carbonyl carbon (δ_C 174.1) of HyLeu and the NH proton (δ_H 7.82) of Aib1, the carbonyl carbon (δ_C 177.9) of Aib1 and the NH proton (δ_H 7.54) of Leu1, the carbonyl carbon (δ_C 176.3) of Leu1 and the NH proton (δ_H 7.77) of Leu2, the carbonyl carbon (δ_C 175.8) of Leu2 and the NH proton (δ_H 7.76) of Aib2, the carbonyl carbon (δ_C 176.0) of Aib2 and the NH proton (δ_H 7.25) of Aib3, the carbonyl carbon (δ_C 177.4) of Aib3 and the NH proton (δ_H 7.57) of β -Ala, and the carbonyl carbon (δ_C 173.5) of β -Ala and the NH proton (δ_H 8.13) of Ala.

In addition, high-resolution ESI tandem mass spectrometry (MS/MS) analysis was performed to confirm the planar structure of 2. The higher energy collisional dissociation experiments for 2 gave most of the b-series product ions at m/z 194.1537, 222.1486, 435.2847, 546.3527, 649.4158, 762.4999, 875.5838, 960.6359, and 1045.6896 in positive ion mode (Figures 3 and S10), allowing the determination of the sequence of the eight N-terminal residues (but not the two C-terminal residues). These product ions of 2 are barely distinguishable from those of 1 (Figure S9), indicating that 1 and 2 have a common substructure from the 4-methyl-2-hexenoic acid moiety to the Aib3 residue. Next, 2 was subjected to HCD experiments in negative ion mode to verify the C-terminal sequence (Figure S11). The product ions at m/z 159.0772 and 88.0406 indicate the presence of β -Ala and Ala at the C-terminus, suggesting that the structure of 2 contains

Table 1. NMR Spectroscopic Data for Leucinostatins A (1) and B (2) in CD₃OH^a

residue	position	leucinostatin A (1)		leucinostatin Y (2)		residue	position	leucinostatin A (1)		leucinostatin Y (2)	
		δ_C type	δ_H (J in Hz)	δ_C type	δ_H (J in Hz)			δ_C type	δ_H (J in Hz)	δ_C type	δ_H (J in Hz)
Δ MHA	1	168.2, C		168.3, C		Leu1	1	176.9, C		176.3, C	
	2	120.9, CH	6.31, d (14.8)	120.8, CH	6.31, d (14.6)		2	56.0, CH	4.02, m	55.4, CH	4.06, m
	3	154.4, CH	6.84, dd (8.0, 14.8)	154.4, CH	6.82, dd (8.0, 14.6)		3	40.9, CH ₂	1.61, m	40.7, CH ₂	1.62, m
	4	39.6, CH	2.33, m	39.6, CH	2.32, m				1.81, m		1.82, m
	5	30.0, CH ₂	1.45, m	30.0, CH ₂	1.43, m		4	25.9, CH	1.82, m	26.0, CH	1.79, m
	6	12.1, CH ₃	0.91 ^b	12.1, CH ₃	0.91, t (8.0)		5	21.6, CH ₃	0.88, d (6.0)	21.3, CH ₃	0.88, d (6.6)
	7	19.5, CH ₃	1.09, d (6.6)	19.5, CH ₃	1.08, d (6.8)		6	23.3, CH ₃	0.94 ^b	23.5, CH ₃	0.95, d (6.6)
MePro	1	176.1, C		175.9, C		Leu2	NH	7.60, d (6.2)		7.54 ^b	
	2	64.6, CH	4.32, dd (6.4, 10.8)	64.5, CH	4.32, dd (7.0, 10.4)		1	175.9, C		175.8, C	
	3	39.3, CH ₂	1.58, m	39.2, CH ₂	1.54, m		2	56.5, CH	4.01, m	55.4, CH	4.10, m
	4	34.7, CH	2.40, m	34.6, CH	2.40, m		3	40.7, CH ₂	1.68, m	40.6, CH ₂	1.64, m
	5	55.6, CH ₂	3.39, t (10.2)	55.6, CH ₂	3.36, t (9.8)				1.81, m		1.81, m
AHMOD	6	16.8, CH ₃	1.15, d (6.6)	16.8, CH ₃	1.15, d (6.2)	4	25.8, CH	1.80, m	25.7, CH	1.79, m	
	1	176.9, C		176.6, C		5	22.2, CH ₃	0.89, d (6.0)	21.7, CH ₃	0.89, d (6.6)	
	2	55.6, CH	4.20, m	55.6, CH	4.20, m	6	23.1, CH ₃	0.94 ^b	23.5, CH ₃	0.95, d (6.6)	
	3	37.3, CH ₂	1.50, m	37.3, CH ₂	1.58, m	NH	7.81, d (5.8)		7.77, d (4.8)		
	4	28.0, CH	1.79, m	28.1, CH	1.80, m	Aib2	1	176.8, C		176.0, C	
	5	45.1, CH ₂	1.39, m	45.0, CH ₂	1.39, m		2	57.5, C		57.9, C	
	6	66.4, CH	4.15, m	66.5, CH	4.16, m	3	23.4, CH ₃	1.46, s	24.4, CH ₃	1.43, s	
	7	51.0, CH ₂	2.53, dd (4.4, 16.0)	51.0, CH ₂	2.54, dd (4.4, 16.0)	4	27.1, CH ₃	1.50, s	26.2, CH ₃	1.45, s	
	8	212.5, C		212.5, C		NH	7.89, s		7.76, s		
	9	37.5, CH ₂	2.49, m	37.5, CH ₂	2.49, m	Aib3	1	178.5, C		177.4, C	
	10	7.7, CH ₃	1.01, t (7.4)	7.7, CH ₃	1.01, t (7.0)	2	57.8, C		58.0, C		
11	20.2, CH ₃	0.96, d (6.2)	20.1, CH ₃	0.97, d (6.0)	3	23.3, CH ₃	1.46, s	24.4, CH ₃	1.44, s		
NH		8.65, d (5.0)		8.55, d (5.0)	4	27.5, CH ₃	1.49, s	26.3, CH ₃	1.45, s		
HyLeu	1	174.0, C		174.1, C		NH	7.62, s		7.25, s		
	2	61.3, CH	4.17, m	60.6, CH	4.19, m	β -Ala	1	175.9, C		173.5, C	
	3	76.3, CH	3.75, m	76.9, CH	3.69, dd (4.4, 7.2)		2	38.2, CH ₂	2.29, m	36.7, CH ₂	2.49, m
	4	32.1, CH	1.72, m	32.2, CH	1.73, m	3	38.0, CH ₂	3.25, m	38.0, CH ₂	3.44, m	
	5	17.7, CH ₃	1.02, d (6.4)	18.7, CH ₃	1.02, d (6.6)	NH	7.94, dd (5.0, 8.0)		7.57, dd (6.0, 12.2)		
	6	19.9, CH ₃	0.92 ^b	19.7, CH ₃	0.88, d (6.6)	DMPD	1	64.0, CH ₂	3.50, m		
NH		7.88, d (7.0)		7.91, d (6.4)	2		42.2, CH	4.49, m			
Aib1	1	178.1, C		177.9, C		3	18.6, CH ₃	1.24, d (6.6)			
	2	59.4, C		58.1, C		4	44.8, CH ₃	2.99, s			
	3	23.4, CH ₃	1.48 ^b	23.7, CH ₃	1.49, s	5	44.8, CH ₃	2.99, s			
	4	27.2, CH ₃	1.53 ^b	27.1, CH ₃	1.50, s	NH	7.62 ^b				
NH		7.97, s		7.82, s	Ala	1			176.5, C		
						2			49.6, CH	4.35, m	
						3			17.9, CH ₃	1.37, d (7.2)	
						NH				8.13, d (6.4)	

^aAbbreviations: Δ MHA, 4-methyl-2-hexenoic acid; MePro, 4-methylproline; AHMOD, 2-amino-6-hydroxy-4-methyl-8-oxodecanoic acid; HyLeu, β -hydroxyLeucine; Aib, 2-aminoisobutyric acid; Leu, leucine; β -Ala, β -alanine; DMPD, N^1,N^1 -dimethylpropane-1,2-diamine; Ala, alanine. Chemical shifts of ¹H (500 MHz) and ¹³C (125 MHz) NMR spectra of **1** were adjusted with solvent signal. Chemical shifts of ¹H (600 MHz) and ¹³C (150 MHz) NMR spectra of **2** were adjusted with solvent signal. ^bMultiplicity was not determined due to overlapping signals.

Ala instead of the N^1,N^1 -dimethylpropane-1,2-diamine moiety of the C-terminus in **1**.

The absolute configurations of the constituent amino acids in **2** were partially determined by an advanced Marfey's method. Compound **2** was hydrolyzed with 6 M HCl at 80 °C for 12 h. The hydrolysate was derivatized with the advanced Marfey reagents (i.e., the L- and D-forms of N^{α} -(5-fluoro-2,4-

dinitrophenyl)leucineamide [FDLA]) and analyzed using the extracted ion chromatograms obtained by liquid chromatography–mass spectrometry (LC-MS). The absolute configurations of the α -carbons of MePro, HyLeu, and Leu were determined to be the L-form based on the principle that L-FDLA derivatives of these L-amino acids are eluted faster than the D-FDLA derivatives (Figure S13).^{25,26} In addition, L-

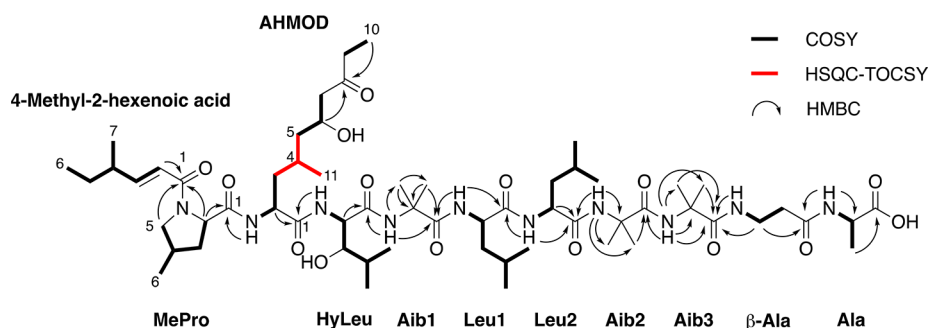


Figure 2. Key correlations of **2** obtained by COSY, HSQC-TOCSY, and HMBC spectroscopies.

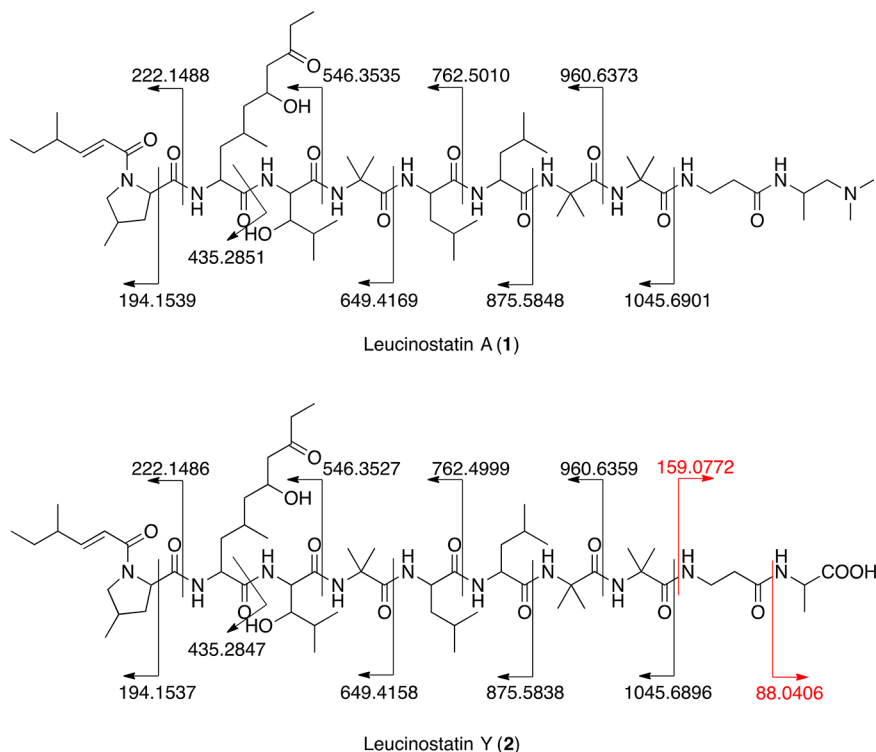


Figure 3. HRESIMS/MS fragmentation of **1** and **2**. The numbers in black indicate the m/z values observed in the positive mode. The numbers in red indicate the m/z values observed in the negative mode.

MePro was revealed to be *cis*-4-methyl-L-proline by the presence of a ROESY cross-peak between H-2 and H-4 of MePro in **2** (Figures S8 and S14). AHMOD is converted to 4-methyl-6-(2-oxobutyl)-2-piperidinecarboxylic acid (MOPA) upon hydrolysis (Figure S15).^{16,27} The LC-MS analysis of the FDLA-derivatized hydrolysate of **2** revealed a signal for (2*S*)-MOPA, indicating the presence of (2*S*)-AHMOD in **2**. The absolute configurations of these amino acids in **2** are identical to those in **1** (Figure S12). Regrettably, the absolute configuration of Ala in **2** could not be determined by the advanced Marfey's method, because L-FDLA-L-Ala and the L-FDLA-β-Ala have the same retention time (t_R) in HPLC analysis (L-FDLA-L-Ala, t_R = 8.5 min; L-FDLA-D-Ala, t_R = 10.5 min; L-FDLA-β-Ala, t_R = 8.5 min). Therefore, the absolute configuration of Ala in **2** was determined by analyzing dipeptides obtained via coupling with Boc-L-Leu and Ala in **2**. The results showed that the hydrolysate of **2** contained both D-Ala and L-Ala as well as β-Ala (Figure S16). These results are most likely an experimental artifact. It is possible that the racemization of Ala during hydrolysis and/or the racemization

of Ala of the C-terminus in **2** during the purification process might occur. Therefore, we isolated **2** without using formic acid as an HPLC solvent additive and further hydrolyzed in 6 M HCl at 38 °C for 48 h. The hydrolysate was coupled with Boc-L-Leu-OSu and analyzed by LC-MS. However, both D-Ala and L-Ala were detected in the hydrolysate of **2**. Thus, the absolute configuration of Ala in **2** remains unclear. Taken together, the structure of **2** was determined to be a new peptaibiotic as shown in Figure 1.

The aldehyde derivative of **2** is thought to be a putative precursor in the biosynthesis of **1**.²⁸ It seems most likely that **2** is generated by oxidation of the aldehyde derivative of **2**. Therefore, the absolute configuration of **2** is considered to be identical to that of **1**. Indeed, some of the amino acids in **2** are shown to have the same absolute configuration as those in **1**, leading to the reasonable prediction that all the chiral centers in **2** exhibit the same absolute configurations as those in **1**.

Leucinostatins display a broad range of biological activities against bacteria, fungi, plants, and cancer cells.^{23,29} Our previous study has shown that a 24 h treatment with **1**

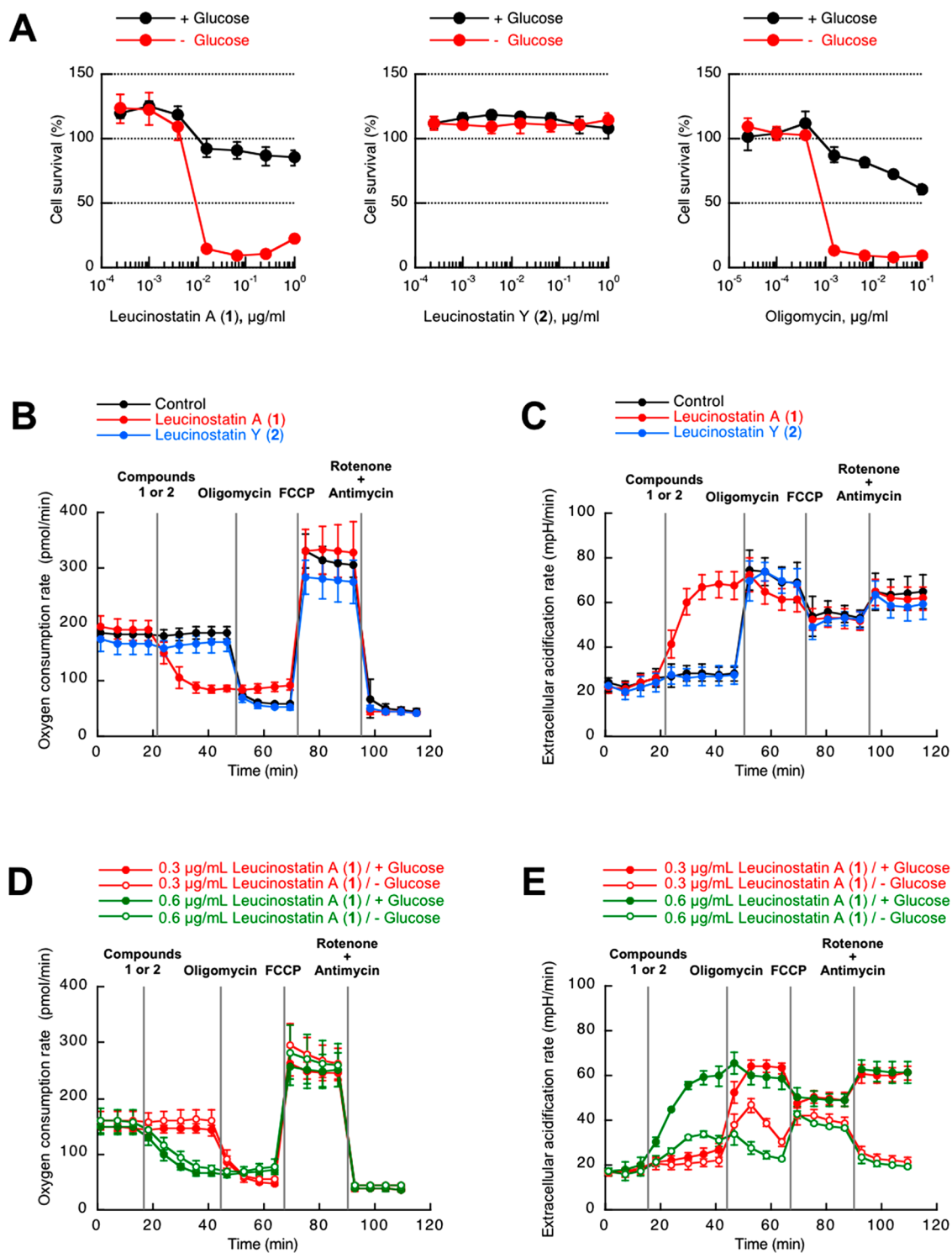


Figure 4. Effect 1 and 2 on the growth of human pancreatic PANC-1 cells and the central metabolism. (A) Preferential cytotoxicity to PANC-1 cells incubated with compounds in DMEM (+ Glucose, black) or GDM (– Glucose, red) for 24 h. Measurement of the oxygen consumption rate (B) and the extracellular acidification rate (C) was performed in Seahorse assay medium supplied with 1 g/L glucose. Measurement of the oxygen consumption rate (D) and the extracellular acidification rate (E) was performed in Seahorse assay medium with/without 1 g/L glucose.

selectively suppresses the growth of human pancreatic cancer cells preferentially under nutrient-deprived conditions compared with that under nutrient-sufficient conditions.¹¹ In this study, we revealed that a 24 h treatment with 1 shows preferential cytotoxicity to human pancreatic cancer PANC-1 cells under glucose-limiting conditions as well as the mitochondrial ATPase inhibitor oligomycin, whereas 2 does

not show any cytotoxicity in the presence or absence of glucose (Figure 4A). These effects of 1 and 2 are exhibited not only in PANC-1 cells but also in human pancreatic cancer BxPC-3, PSN-1, and PK-8 cells (Figure S17). Meanwhile, a 72 h treatment with 1 suppressed the growth of various cancer cells under nutrient-sufficient conditions, while 2 was only slightly active (Table S1). The antimicrobial activities of 1 and 2 were

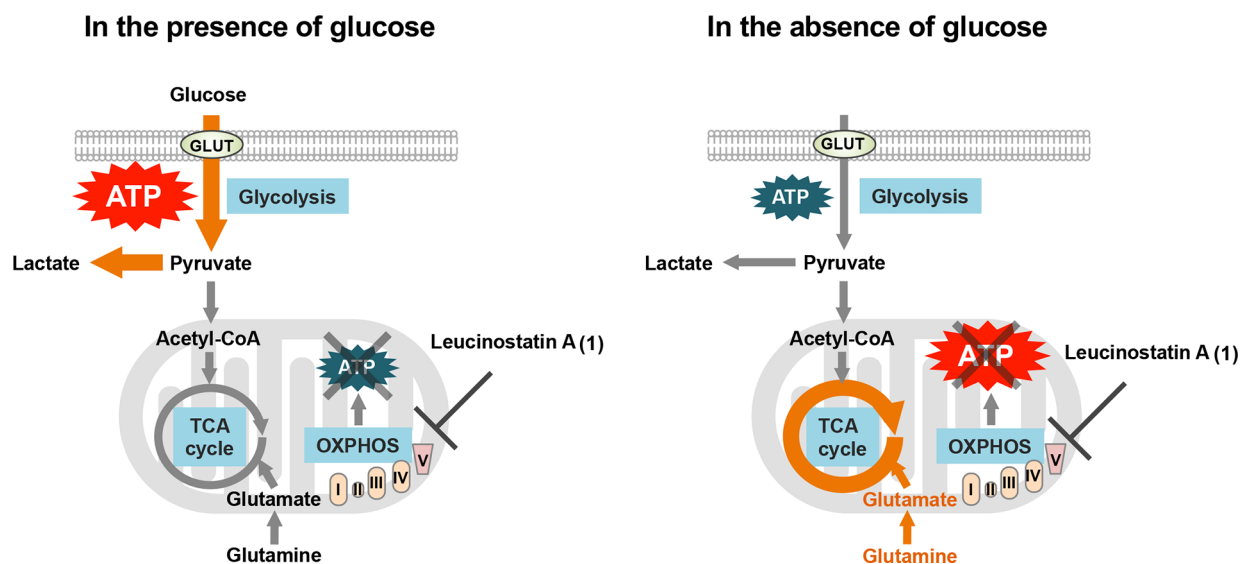


Figure 5. Effect of leucinostatin A (1) on glycolysis and oxidative phosphorylation (OXPHOS).

evaluated by the agar dilution method (Table S2); **1** was active against *Candida* and *Cryptococcus*, while **2** showed much lower activity against the microorganisms tested in this study.

Leucinostatin A (**1**) inhibits mitochondrial respiration by inhibition of mitochondrial ATPase and by uncoupling oxidative phosphorylation.^{30–33} To investigate the effect of **1** and **2** on the mitochondrial respiration of PANC-1 cells, we evaluated the oxygen consumption rate as an indicator of mitochondrial respiration using a Seahorse XFe96 analyzer. The mitochondrial ATPase inhibitor oligomycin decreases the oxygen consumption rate in PANC-1 cells (Figure 4B). Conversely, the oxidative phosphorylation uncoupler *p*-trifluoromethoxyphenylhydrazine (FCCP) increases the oxygen consumption rate. Treatment with **1** significantly decreases the oxygen consumption rate like an oligomycin, indicating that **1** acts as an inhibitor of mitochondrial ATPase in PANC-1 cells. In contrast, treatment with **2** has little effect on the oxygen consumption rate. Next, we measured the extracellular acidification rate as an indicator of glycolysis. Predictably, **1**, like oligomycin, increases the extracellular acidification rate, whereas **2** has little influence on the extracellular acidification rate (Figure 4C). These results indicate that the *N*¹,*N*¹-dimethylpropane-1,2-diamine moiety in **1** plays an important role in the inhibition of mitochondrial ATPase and preferential cytotoxicity under glucose starvation. We also investigated the relationship between the inhibition of mitochondrial function and preferential cytotoxicity under glucose-limiting conditions. The oxygen consumption rate is decreased by 0.6 μg/mL **1**, in the presence or absence of glucose (Figure 4D). Although 0.6 μg/mL **1** significantly increases the extracellular acidification rate in the presence of glucose, 0.6 μg/mL **1** barely increases the extracellular acidification rate in the absence of glucose (Figure 4E). These data indicate that the suppression of mitochondrial respiration by **1** under glucose-sufficient conditions promotes ATP production through glycolysis. However, **1** does not activate glycolysis under glucose-deprived conditions. Therefore, glucose-sufficient cells can survive in the presence of **1**, whereas glucose-deprived cells cannot (Figure 5).

In conclusion, we have discovered a new metabolite produced by the fungal strain 40-H-28. This strain was

isolated from the synnema formed on *M. japonensis* Scott collected in Japan and has been identified as the entomoparasitic fungus *P. lilacinum* 40-H-28. We found that *P. lilacinum* strain 40-H-28 produces a new leucinostatin named leucinostatin Y (**2**), together with leucinostatin A (**1**). The ¹H and ¹³C NMR have been assigned for the first time. Leucinostatins belong to a class of peptaibiotics that are defined as fungal peptides containing α-monosubstituted α-amino acids such as Aib, and **2** was found to be a peptaibiotic comprising 10 α-amino acids (including unusual amino acids). The spectroscopic data for **2** revealed that it has the same structure as **1** but with the *N*¹,*N*¹-dimethylpropane-1,2-diamine moiety at the C-terminus substituted with Ala. There are 24 known leucinostatin structures,²¹ all of which have a 1,2-diaminopropane moiety at the C-terminus. Compound **2**, which lacks the 1,2-diaminopropane moiety, represents the first leucinostatin of its type. In addition, **1** shows preferential cytotoxicity under glucose-limiting conditions and inhibition of mitochondrial respiration, whereas **2** does not show any cytotoxicity or influence on mitochondrial function. Thus, the *N*¹,*N*¹-dimethylpropane-1,2-diamine moiety of **1** plays an important role in its biological activities. The druggability of **2** is poor because the pharmacological activity is weak. However, information regarding the structure–activity relationship of **2** obtained in our study may be quite useful in the development of new leucinostatin derivatives.

Recently, **1** was found to suppress the growth of prostate cancer cells in a coculture system with prostate stromal cells through reduction of insulin-like growth factor-I signaling.^{34,35} In the tumor microenvironment, tumor cells are exposed to insufficient nutrient supply and are closely related to normal cells such as stromal cells. Therefore, leucinostatins may be promising anticancer agents that target tumor microenvironments.

EXPERIMENTAL SECTION

General Experimental Procedures. NMR spectra were acquired on a ECZ600R (JEOL, Tokyo, Japan) and an AVANCE III 500 (Bruker, Billerica, MA, USA). Chemical shifts are referenced to the residual solvent peak in the NMR solvent. Infrared (IR) spectra were recorded on an FT-710 Fourier-transform infrared spectrophotometer (Horiba, Kyoto, Japan). UV absorption spectra were determined

using a U-3210 spectrophotometer (Hitachi, Tokyo, Japan). Optical rotation was measured using a 241 polarimeter (PerkinElmer, Waltham, MA, USA). HRESIMS and MS/MS spectra were recorded on a Q Exactive hybrid quadrupole-Orbitrap mass spectrometer (Thermo Fisher Scientific, San Jose, CA, USA) and an LTQ Orbitrap XL hybrid iontrap-Orbitrap mass spectrometer (Thermo Fisher Scientific), respectively. LC-MS was performed by a Q Exactive hybrid quadrupole-Orbitrap mass spectrometer with an UltiMate 3000 HPLC system (Thermo Fisher Scientific).

Isolation and Taxonomic Analysis of Strain 40-H-28. The fungus strain 40-H-28 was isolated from the synnema formed on *M. japonensis* Scott that was collected at Yokohama City, Kanagawa Prefecture, Japan, on August 3, 2013. The entomoparasitic fungus with synnemata from an imago of *M. japonensis* was first reported by Kobayasi and designated as *Isaria macroscyticola* (Tutikamemusitake).²² The morphological characteristics of the *I. macroscyticola* are similar to those of strain 40-H-28. However, strain 40-H-28 has verticillate conidiophores and chains of ovoid conidia that are characteristic of *P. lilacinum* (see graphical abstract, in which the hyphae and conidia are stained with phenol cotton blue). Ebehard et al. showed that *P. cf. lilacinum* infected *Edessa rufomarginata* (hemiptera, pentatomidae) and formed synnemata.³⁶ The total genomic DNA was isolated from the cell body of the strain 40-H-28 grown on potato dextrose agar (Becton, Dickinson and Company, Sparks, MD, USA) at 25 °C. The ITS-5.8S gene sequence of strain 40-H-28 was found to be 100% identical to the registered sequences of *P. lilacinum* found in the DDBJ/EMBL/GenBank databases. The nucleotide sequence of the ITS-5.8S rDNA region of strain 40-H-28 was deposited in the DDBJ/EMBL/GenBank databases with the accession number LC416799. Thus, the isolated strain 40-H-28 was identified as *P. lilacinum* based on its morphological and phylogenetic analysis.

Fermentation and Isolation of Leucinostatins. A slant culture of *P. lilacinum* 40-H-28 was inoculated into a 500 mL Erlenmeyer flask containing seed medium (100 mL) consisting of soybean meal (2%) and mannitol (3%). The flask was incubated at 25 °C for 4 days on a rotary shaker operating at 220 rpm. Aliquots (1 mL) of this seed culture were transferred into 500 mL Erlenmeyer flasks containing production medium (100 mL) having the same ingredients as the seed medium. The flasks were cultured at 25 °C for 6 days on a rotary shaker operating at 220 rpm.

The culture filtrate obtained from the fermented broth (16 L) was applied to a Diaion HP-20 column (2 L, Mitsubishi Chemical, Tokyo, Japan). After washing with 50% aqueous acetone, the fractions containing the active compounds were eluted with acetone. The active fractions were concentrated *in vacuo*, applied to a silica gel 60 column (Merck, Darmstadt, Germany), and eluted with CHCl₃–MeOH (1:1). Then, the active fractions were concentrated under reduced pressure to yield a brown material. The material was dissolved in CHCl₃–MeOH (1:1), applied to a Sephadex LH-20 column (GE Healthcare, Little Chalfont, UK), and eluted with CHCl₃–MeOH (1:1). The fractions containing the leucinostatins were further purified by preparative HPLC [Capcell Pak C₁₈ UG-120 (5 μm 30 × 250 mm, Shiseido, Tokyo, Japan); flow rate, 20 mL/min; solvent gradient, 5–95% aqueous CH₃CN containing 0.1% formic acid, linear gradient]. **1** and **2** were eluted at 28–30 min and 36–37 min, respectively. These fractions were concentrated under reduced pressure to give pure **1** (46.4 mg) and **2** (18.8 mg). Furthermore, LC-MS analysis revealed that several leucinostatins in addition to **1** and **2** were present in the culture broth of *P. lilacinum* 40-H-28 and the MeOH extract of mycelia (Figure S18).

Leucinostatin Y (2): colorless, amorphous solid; mp 107–111 °C; [α]_D²⁴ –24.0 (c 1.77, MeOH); UV (MeOH) λ_{\max} (log ϵ) 205 (4.45), 223 (sh 4.27) nm; IR (KBr) ν_{\max} 3332, 2960, 1658, 1537, 1441, 1387, 1365, 1293, 1223 cm⁻¹; HRESIMS m/z 1205.7758 (calcd for C₆₀H₁₀₅N₁₀O₁₅, 1205.7755).

Determination of Absolute Configurations of Amino Acids. The absolute configurations of the α -carbons of MePro, AHMOD, HyLeu, and Leu were determined by the advanced Marfey's method.^{25,26} The leucinostatins (0.1 mg) were hydrolyzed with 0.5

mL of 6 M HCl at 80 °C for 12 h. The reaction mixture was then evaporated to dryness under reduced pressure, and the resulting residue was dissolved in 120 μL of water. Subsequently, two vials were each charged with 50 μL of the hydrolysate and 20 μL of 1 M NaHCO₃. Then, 50 μL of 10 mg/mL D-FDLA (Tokyo Chemical Industry, Tokyo, Japan) in acetone was added to one of the two vials, and an equivalent proportion of L-FDLA in acetone was added to the other vial. The two reaction vials were stirred at 37 °C for 60 min. Then, 20 μL of 1 M HCl was added to each vial, and the two reaction mixtures were diluted 100-fold with 50% aqueous CH₃CN. A 5 μL aliquot of each diluent was injected into the LC-MS apparatus. LC-MS analyses were performed under the following conditions: column, Capcell Pak C18 UG120 (3 μm, 2.0 × 50 mm, Shiseido); flow rate, 0.3 mL/min; solvent gradient, 20–60% aqueous CH₃CN containing 0.1% formic acid, linear gradient; mass spectrometer, positive ion; detection, protonated molecules, m/z 424.1827 ± 0.0013 for MePro, m/z 442.1932 ± 0.0013 for HyLeu, m/z 426.1983 ± 0.0013 for Leu, and m/z 508.2402 ± 0.0015 for MOPA. Because AHMOD is converted to MOPA upon hydrolysis, MOPA was detected instead of AHMOD.

To determine the absolute configurations of Ala, the Boc-L-leucine hydroxysuccinimide ester (Boc-L-Leu-OSu) was coupled with three kinds of Ala (D-ALA, L-Ala, and β-Ala) to yield the dipeptides Boc-L-Leu-D/L/β-Ala, respectively. Briefly, leucinostatins (0.1 mg) were hydrolyzed with 0.5 mL of 6 M HCl at 38 °C for 48 h and the reaction mixture was concentrated under reduced pressure to dryness. Subsequently, to 80 μL of hydrolysate dissolved in 120 μL of water were added 20 μL of 1 M NaHCO₃ and 100 μL of Boc-L-Leu-OSu (40 mg/mg, 1,4-dioxane). The reaction mixture was then stirred at 25 °C for 12 h, and 20 μL of 1 M HCl was added to neutralize. The reaction mixture was diluted 200-fold with 50% aqueous CH₃CN, and 5 μL of the diluent was injected into the LC-MS. The LC-MS analyses were performed under the same conditions as those used in the advanced Marfey's method. The dipeptides were monitored using extracted ion chromatograms for the cationized molecule, m/z 325.1734 ± 0.0016 (M + Na)⁺.

Cell Culture. Human pancreatic cancer PANC-1, BxPC-3, and PSN1 cells were obtained from the American Type Culture Collection (Rockville, MD, USA), and PK-8 cells were obtained from Riken Cell Bank (Ibaraki, Japan). Cells were grown at 37 °C with 5% CO₂ in Dulbecco's modified Eagle medium (DMEM; Nissui, Tokyo, Japan) supplemented with 10% fetal bovine serum (FBS; Cosmo Bio, Tokyo, Japan), 10 000 units/L penicillin G, and 10 mg/mL streptomycin.

Glucose starvation was achieved by culturing cells in glucose-deprived medium (GDM). The GDM composition was 265 mg/L CaCl₂·H₂O, 400 mg/L KCl, 200 mg/L MgSO₄·7H₂O, 6400 mg/L NaCl, 163 mg/L NaH₂PO₄·2H₂O, 0.1 mg/L Fe(NO₃)₃·9H₂O, MEM vitamin solution (Invitrogen, Carlsbad, CA, USA), MEM amino acids solution (Invitrogen), 292 mg/L L-glutamine, 42 mg/L L-serine, 30 mg/L L-glycine, 110 mg/L sodium pyruvate, 5 mg/L phenol red, 10 000 units/L penicillin G, 10 mg/L streptomycin, 25 mmol/L HEPES buffer (pH 7.4), and 10% dialyzed FBS. The final pH was adjusted to 7.4 with 10% NaHCO₃.

Preferential Cytotoxicity in Glucose-Deprived Conditions. Cells (2.5 × 10⁴ cells/well) in 96-well plates were cultured in DMEM for 24 h. The cells were then washed with phosphate-buffered saline (–), and the medium was replaced with either fresh DMEM (+ glucose) or GDM (– glucose). Leucinostatins were then added to the wells, and the cells were cultured for 24 h. Then, the medium was replaced with DMEM containing 0.5 mg/mL 3-(4,5-dimethylthiazol-2-yl)-2,5-diphenyltetrazolium bromide (MTT; Sigma-Aldrich) and incubated at 37 °C for 4 h. After incubation, cells were supplemented with 20% sodium dodecyl sulfate and incubated at 37 °C for 12 h. Absorbance was measured at 570 nm using a spectrophotometer.

Measurement of Oxygen Consumption Rate and Extracellular Acidification Rate. Cellular mitochondrial function was measured using a Seahorse XF Cell Mito stress test kit (Agilent Technologies, Santa Clara, CA, USA). This kit can be used for measuring key parameters of mitochondrial function (basal

respiration, ATP production, proton leak, maximal respiration, and nonmitochondrial respiration). The testing was performed in accordance with the protocol provided in the supplier's manual. Briefly, 2×10^4 PANC-1 cells were plated onto XF cell culture plates in DMEM and incubated at 37 °C with 5% CO₂ overnight. Cells were washed with assay medium (Seahorse XF base medium containing 1 g/L glucose, 1 mM sodium pyruvate, and 2 mM GlutaMax-1 (Thermo Fisher Scientific)) and replaced with assay medium. The plate was placed at 37 °C in a CO₂-free incubator for 30 min and then loaded into a Seahorse XFe96 analyzer (Agilent Technologies). The oxygen consumption rate and extracellular acidification rate were monitored in real-time throughout the assay. Leucicostatin, 1 μM oligomycin, 1 μM FCCP, and 0.5 μM rotenone plus 0.5 μM antimycin were sequentially injected into each well. Data points represent the mean rates of each measurement cycle, which consisted of 2 min mixing time, followed by 3 min data acquisition (20 or 21 cycles in total).

■ ASSOCIATED CONTENT

● Supporting Information

The Supporting Information is available free of charge on the ACS Publications website at DOI: [10.1021/acs.jnatprod.8b00839](https://doi.org/10.1021/acs.jnatprod.8b00839).

Additional information (PDF)

■ AUTHOR INFORMATION

Corresponding Author

*Phone: +81-55-924-0601. Fax: +81-55-922-6888. E-mail: imomose@bikaken.or.jp.

ORCID

Isao Momose: [0000-0002-9867-3881](https://orcid.org/0000-0002-9867-3881)

Notes

The authors declare no competing financial interest.

■ ACKNOWLEDGMENTS

This work was financially supported by JSPS KAKENHI Grant Number 15K01811. We thank Dr. H. Abe and Dr. T. Watanabe (BIKAKEN) for providing synthetic leucicostatin A, Dr. H. Hashizume (BIKAKEN) for determination of absolute configuration of amino acids, Dr. T. Kudo (PRIMETECH) and Dr. S. Atsumi (BIKAKEN) for the extracellular flux analyzer-based analysis, Ms. Y. Shibuya (BIKAKEN) for evaluation of the antimicrobial activity, and Ms. S. Kakuda and Ms. K. Hitosugi (BIKAKEN) for technical assistance.

■ REFERENCES

- (1) Vaupel, P.; Kallinowski, F.; Okunieff, P. *Cancer Res.* **1989**, *49*, 6449–6465.
- (2) Brown, J. M.; Giaccia, A. J. *Cancer Res.* **1998**, *58*, 1408–1416.
- (3) Izuishi, K.; Kato, K.; Ogura, T.; Kinoshita, T.; Esumi, H. *Cancer Res.* **2000**, *60*, 6201–6207.
- (4) Lee, A. S. *Cancer Res.* **2007**, *67*, 3496–3499.
- (5) Wang, M.; Kaufman, R. J. *Nat. Rev. Cancer* **2014**, *14*, 581–597.
- (6) Kunimoto, S.; Lu, J.; Esumi, H.; Yamazaki, Y.; Kinoshita, N.; Honma, Y.; Hamada, M.; Ohsono, M.; Ishizuka, M.; Takeuchi, T. *J. Antibiot.* **2003**, *56*, 1004–1011.
- (7) Kunimoto, S.; Someno, T.; Yamazaki, Y.; Lu, J.; Esumi, H.; Naganawa, H. *J. Antibiot.* **2003**, *56*, 1012–1007.
- (8) Lu, J.; Kunimoto, S.; Yamazaki, Y.; Kaminishi, M.; Esumi, H. *Cancer Sci.* **2004**, *95*, 547–552.
- (9) Park, H. R.; Furihata, K.; Hayakawa, Y.; Shin-ya, K. *Tetrahedron Lett.* **2002**, *39*, 6941–6945.
- (10) Park, H. R.; Tomida, A.; Sato, S.; Tsukumo, Y.; Yun, J.; Yamori, T.; Hayakawa, Y.; Tsuruo, T.; Shin-ya, K. *J. Natl. Cancer Inst.* **2004**, *96*, 1300–1310.
- (11) Momose, I.; Ohba, S.; Tatsuda, D.; Kawada, M.; Masuda, T.; Tsujiuchi, G.; Yamori, T.; Esumi, H.; Ikeda, D. *Biochem. Biophys. Res. Commun.* **2010**, *392*, 460–466.
- (12) Bérdy, J. *J. Antibiot.* **2012**, *65*, 385–395.
- (13) Isaka, M.; Kittakoop, P.; Kirtikara, K.; Hywel-Jones, N. L.; Thebtaranonth, Y. *Acc. Chem. Res.* **2005**, *38*, 813–823.
- (14) Molnár, I.; Gibson, D. M.; Krasnoff, S. B. *Nat. Prod. Rep.* **2010**, *27*, 1241–1275.
- (15) Degenkolb, T.; Berg, A.; Gams, W.; Schlegel, B.; Gräfe, U. *J. Pept. Sci.* **2003**, *9*, 666–678.
- (16) Fukushima, K.; Arai, T.; Mori, Y.; Tsuboi, M.; Suzuki, M. *J. Antibiot.* **1983**, *36*, 1613–1630.
- (17) Rossi, C.; Tuttobello, L.; Ricci, M.; Casinovi, C. G.; Radics, L. *J. Antibiot.* **1987**, *40*, 130–133.
- (18) Radics, L.; Kajtar-Peredy, M.; Casinovi, C. G.; Rossi, C.; Ricci, M.; Tuttobello, L. *J. Antibiot.* **1987**, *40*, 714–716.
- (19) Cerrini, S.; Lamba, D.; Scatturin, A.; Ughetto, G. *Biopolymers* **1989**, *28*, 409–420.
- (20) Isogai, A.; Nakayama, J.; Takayama, S.; Kusai, A.; Suzuki, A. *Biosci., Biotechnol., Biochem.* **1992**, *56*, 1079–1085.
- (21) Martinez, A. F.; Moraes, L. A. *J. Antibiot.* **2015**, *68*, 178–184.
- (22) Kobayasi, Y. *Sc. Rep. T.B.D. Sect. B* **1941**, *5*, 53–260.
- (23) Arai, T.; Mikami, Y.; Fukushima, K.; Utsumi, T.; Yazawa, K. *J. Antibiot.* **1973**, *26*, 157–161.
- (24) Abe, H.; Ouchi, H.; Sakashita, C.; Kawada, M.; Watanabe, T.; Shibasaki, M. *Chem. - Eur. J.* **2017**, *23*, 11792–11796.
- (25) Harada, K.; Fujii, K.; Hayashi, K.; Suzuki, M.; Ikai, Y.; Oka, H. *Tetrahedron Lett.* **1996**, *37*, 3001–3004.
- (26) Hashizume, H.; Iijima, K.; Yamashita, K.; Kimura, T.; Wada, S.; Sawa, R.; Igarashi, M. *J. Antibiot.* **2018**, *71*, 129–134.
- (27) Mori, Y.; Tsuboi, M.; Suzuki, M.; Fukushima, K.; Arai, T. *J. Antibiot.* **1982**, *35*, 543–544.
- (28) Wang, G.; Liu, Z.; Lin, R.; Li, E.; Mao, Z.; Ling, J.; Yang, Y.; Yin, W. B.; Xie, B. *PLoS Pathog.* **2016**, *12*, No. e1005685.
- (29) Lucero, A. H.; Ravizzini, A. R.; Vallejos, H. R. *FEBS Lett.* **1976**, *68*, 141–144.
- (30) Lloyd, D.; Edwards, S. W. *Biochem. J.* **1977**, *162*, 581–590.
- (31) Schmitt, M.; Rittinghaus, K.; Scheurich, P.; Schwulera, U.; Dose, K. *Biochim. Biophys. Acta, Biomembr.* **1978**, *509*, 410–418.
- (32) Reed, P. W.; Lardy, H. A. *J. Biol. Chem.* **1975**, *250*, 3704–3708.
- (33) Fukushima, K.; Arai, T.; Mori, Y.; Tsuboi, M.; Suzuki, M. *J. Antibiot.* **1983**, *36*, 1606–1612.
- (34) Kawada, M.; Inoue, H.; Ohba, S.; Masuda, T.; Momose, I.; Ikeda, D. *Int. J. Cancer* **2009**, *126*, 810–818.
- (35) Abe, H.; Kawada, M.; Sakashita, C.; Watanabe, T.; Shibasaki, M. *Tetrahedron* **2018**, *74*, 5129–5137.
- (36) Eberhard, W.; Pacheco-Esquivel, J.; Carrasco-Rueda, F.; Christopher, Y.; Gonzalez, C.; Ramos, D.; Urbina, H.; Blackwell, M. *Mycologia* **2014**, *106*, 1065–1072.